Journal of Magnetic Resonance Open 6–7 (2021) 100012

Contents lists available at ScienceDirect

Journal of Magnetic Resonance Open

journal homepage: www.elsevier.com/locate/jmro

Concept paper

# Application of $^1$H proton NMR relaxometry to building materials – A review

Sarah Mandy Nagel[a,*], Christoph Strangfeld[a], Sabine Kruschwitz[a,b]

[a] Bundesanstalt für Materialforschung und -prüfung (BAM), Unter den Eichen 87, Berlin 12205, Germany
[b] Technische Universität Berlin, Gustav-Meyer-Allee 25, Berlin 13355, Germany

ARTICLE INFO

*Keywords:*
NMR relaxometry
Building materials
Natural stones
Relaxation times
Surface relaxivities
Moisture
Pore space characterization

ABSTRACT

Since nuclear magnetic resonance with focus on $^1$H protons is highly sensitive to pore filling fluids, it is nowadays often applied for the investigation of porous media. Mainly in materials research and especially in the field of non-destructive testing in civil engineering it is increasingly used. Scientific questions about and based on NMR meanwhile cover a broad spectrum.

To give an overview, we have reviewed various studies dealing with the determination of moisture contents and parameters such as the pore-size distribution, surface relaxivity, porosity, etc. In some papers, the monitoring of moisture transport in connection with degradation processes or admixtures was the main objective. In other papers, NMR was used for pore space analysis or even applied on site to assess the state of conservation of cultural heritage. Building materials that have been investigated in the presented studies are for example cement, concrete, woods, sandstones etc.

In this paper, short descriptions and the significant results of the reviewed articles are summarized and their measurement problems and discrepancies are pointed out. A special feature of this review article is the concise tabular compilation of determined $T_1$ and $T_2$ relaxation times, as well as of surface relaxivity values for various materials and components. Finally, relevant aspects are summed up and conclusions about the increasing potential of NMR relaxometry for investigations of porous building materials are drawn, followed by an outlook about future applications and the need for technical development.

## 1. Introduction

The physical phenomenon of nuclear magnetic resonance (NMR) in bulk material was discovered in the 1940s by Bloch [1] and Purcell et al. [2]. However, the origin of NMR goes back further and lies in the development of the spin concept in the 1920s and the discovery of the proton's magnetic moment [3]. First NMR applications were limited to physical and chemical experiments in laboratory (e.g. carbon and silicon chemistry)[4]. While most chemists applied continuous wave NMR, the physicists started to focus on pulse NMR with the aim of analyzing solids. Soon, the measurement of relaxation times with pulse NMR became an important issue for oil exploration. As described in Woessner [5] and Varian [6], the methodology NMR logging (earlier known as nuclear magnetism logging) was introduced in the early 1950s. Later, NMR started to be applied in biochemistry and materials research [3,7–9]. A list of the first investigated non-metallic solids may be found in Andrew [9].

In the early 1980s, NMR was finally enhanced to high-resolution solid-state NMR and could be applied on cementitious materials with an additional focus on hydration processes [10–12]. Since then, there has been an intensive development as a response to the steadily growing demand on cement and concrete research. Nowadays, particularly the NMR relaxometry with focus on $^1$H protons is increasingly used in civil engineering; especially in non-destructive testing. Besides material and pore space characterization, the analysis of degradation phenomena (e.g. microfractures, disintegration and alcali-silica reaction) and other effects of environmentally-induced damages are of high significance [13–15]. Moreover, current topics are also stone conservation within the scope of cultural heritage [16,17], quality assessment of concrete coating systems and the influence of steel reinforcement on on-site NMR measurements [18]. Therefore, there is an obvious need for an updated overview about possible applications as well as about technical and methodical restrictions for the use on building materials.

The review article points out the objectives of the research done so far and sums up various application restrictions. We refer to numerous studies of proton NMR relaxometry applied to different kinds of porous building materials. The reviewed papers deal for example with hydrated building materials as well as with fresh pastes, natural stones, etc. Thus, several studies focus on moisture transport, determination of pore-size distributions (PSD) or corresponding NMR parameters such

* Corresponding author.
*E-mail address:* sarah-mandy.nagel@bam.de (S.M. Nagel).

https://doi.org/10.1016/j.jmro.2021.100012
Received 8 September 2020; Received in revised form 1 December 2020; Accepted 6 February 2021

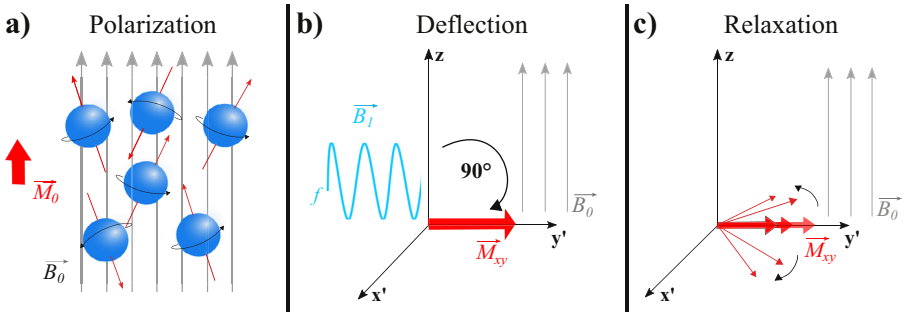


**Fig. 1.** The three main steps of the NMR principle: Polarization (a), deflection (b) and relaxation of protons (c). *Source:* own presentation.

as the surface relaxivity. Some authors also present results regarding related process limitations when using $^1$H NMR relaxometry. Most of these experiments were conducted in laboratories, while only few results were collected in the field. In this article, a variety of possible set-ups using NMR devices such as single-sided or bench-top devices, spectrometers and drill core analyzing instruments is covered.

To obtain an overview about the various reviewed studies, we sorted their relevant results according to the materials under investigation and related to the scientific questions. For better comparison, we compiled the determined values of transversal and longitudinal relaxation times as well as the surface relaxivities and summarized them in Section 4.

Our paper is structured as follows:

- First, the theoretical background is presented.
- Then, the following main sections discuss the current technical developments, applications, and the related restrictions and discrepancies regarding NMR measurements in porous building materials.
- Finally, the applicability and significance of NMR for non-destructive testing in civil engineering and future topics are summarized and discussed.

## 2. Physical principle of nuclear magnetic resonance

The geophysical method NMR is based on the interaction of atomic nuclei with magnetic fields. Depending on the technical set-up and especially on the magnetic field strength, the method can be divided into high- and low-resolution applications. High-resolution NMR (spectroscopy) enables the analysis of chemical properties and structural information on molecular basis such as bonding types. Nevertheless, spectroscopy requires strongly homogeneous magnetic fields with closed magnet constructions so that the sample size is often limited to a few grams. To achieve strong field strengths (e.g. in excess of 2.3 T), large superconducting magnets are needed [19]. Thus, this review mainly focuses on low-resolution NMR (especially relaxometry applications) which allows the investigation of larger samples or even of building constructions on site. Low-resolution NMR is often also named dynamic NMR and includes both relaxometry and diffusometry measurements [10]. NMR diffusometry measurements are based on field gradients and aim to study diffusion processes and to determine self-diffusion coefficients [20,21]. As explained by Blümich et al. [22], low-field NMR uses static magnetic fields in the order of one Tesla or less and hence operates at frequencies up to 50 MHz. In contrast to NMR spectroscopy, NMR relaxometry provides information at a larger scale e.g. about pore structures and fluid transport and is therefore typically used to determine the water content, porosity as well as permeability. NMR relaxometry is also applied for describing pore spaces of porous materials, composites and solids [10,23].

In general, the NMR method is applicable to various NMR-active nuclei that have a magnetic dipole moment caused by their nuclear angular moment or nuclear spin [8,22]. The standard isotope to be investigated by single-sided NMR is $^1$H, since it has a large magnetic moment and therefore produces a high NMR signal [8,24]. The simplified principle of NMR is presented in Fig. 1. In a static magnetic field $B_0$ (longitudinal axis, z-axis), the nuclei or spins align with $B_0$ and start to precess around the field axis with their specific Larmor frequency $\lambda$. This alignment process (polarization) leads to a net bulk magnetization $M_0$ parallel to $B_0$. The time it takes to polarize all spins, can be measured and is specified as the longitudinal relaxation time $T_1$ (see Eq. (1)). Furthermore, at equilibrium, the magnitude of $M_0$ is proportional to the atomic nuclei content in the measuring volume [25]. In the case of a water-filled, but itself hydrogen-free pore matrix, the magnitude of $M_0$ provides the water content of the investigated volume and in fully saturated media, even the porosity may be obtained (calibration needed).

After polarization, a secondary magnetic field $B_1$ perpendicular to $B_0$ is turned on. When $B_1$ oscillates with the precession frequency, the nuclear magnetization can be tilted into the transverse plane (x'-y' plane, orientation of $B_1$) due to the occurring resonance effect. Subsequently, $B_1$ is turned off and the spins start to dephase (relaxation). Therefore, the net magnetization $M_{xy}$ decreases and a decaying signal can be measured in the transverse plane. The time constant of this relaxation process is called the transversal relaxation time $T_2$ (see Eq. (2)).

$$M_z(t) = M_0\left(1 - e^{\frac{-t}{T_1}}\right) \tag{1}$$

$$M_{xy}(t) = M_{0_{xy}}\left(e^{\frac{-t}{T_2}}\right) \tag{2}$$

where $M$ is the magnetization; $t$ is the time and $T$ is the relaxation time.

Both above described time constants are measurable and normally related to mono- or multi-exponential signals. In addition to the magnetization's magnitude, the decaying relaxation processes themselves provide further parameters to analyze the pore spaces and the pore filling fluids.

In the following section, the authors give a short description of relaxation within porous media. More theoretical details and explanations of the NMR basics and typically used pulse sequences can be found in [8,20,22,25]. A comparison of $T_1$ and $T_2$ measurements as well as their advantages and disadvantages is given by [26]. Details on the development of multidimensional NMR methodology having more than one measurand in contrast to conventional NMR relaxation and diffusion experiments, are given by Song [7], Stapf and Han [21]. They give information on NMR in porous media and describe various multidimensional relaxation and diffusion measurement experiments in detail (e.g. diffusion-relaxation or relaxation correlation).

### 2.1. Relaxation process in porous media

When NMR is applied to building materials such as cement based or natural materials, measurable protons can be found in both their chemical structures and in the pore filling fluid. Since the chemically and physically bonded water has much shorter relaxation times compared to porous trapped liquid water, the latter mainly contributes to the NMR signal. However, the relaxation process described in the previous section is influenced not only by the molecules themselves, but by their environment as well [22]. This environment is defined by the pore shapes, their connectivity, sizes and the mineralogical composition.

While synthetic materials are often characterized by well-defined pores and sometimes even periodic structures, natural materials may have irregular pore shapes and sizes. In building materials, which may include both natural and synthetic components such as cement, concrete, rocks or partially synthetic fibres, even both types of pore systems co-exist [22].

A first model to explain relaxation processes in pores (biological cells) was presented by Brownstein and Tarr [27]. In the proposed theory, the relaxation process in pores was firstly described as a multi-exponential decaying signal in contrast to the mono-exponential nature of bulk water's relaxation. Brownstein and Tarr [27] explained the phenomenon as a consequence of size and shape of the spatial environment. The main causes that lead to a much faster relaxation than in bulk water are the natural diffusion of molecules, possible collisions with the pore wall and diffusion caused by the influence of paramagnetic minerals on the pore surface or by the inhomogeneity of $B_0$. Therefore, a proton crossing through a pore may pass two different relaxation regimes, the surface and the bulk relaxation regime [22]. Within the bulk relaxation regime, relaxing molecules do not collide with the pore wall and are constantly surrounded by the bulk fluid. The surface relaxation regime though refers to relaxation of molecules that diffuse close to the pore wall and are affected by paramagnetic impurities.

Considering that the longitudinal relaxation is insensitive to diffusion effects (self-diffusion) caused by internal and external magnetic field gradients, for fluids in pores (especially rock pores) a longitudinal relaxation rate ($\frac{1}{T_1}$) may be divided into two components [25]. On the contrary, the transverse relaxation rate ($\frac{1}{T_2}$) may be described by three components including the above named diffusion relaxation rate [8]. The corresponding equations of relaxation rates may be described as follows:

$$\frac{1}{T_{1,2}} = \frac{1}{T_{1,2Bulk}} + \frac{1}{T_{1,2Surface}} + \frac{1}{T_{2Diffusion}} \tag{3}$$

with $T_{Bulk}$ as the relaxation time of the pore fluid without influence of the environment; $T_{Surface}$ as the relaxation time of the pore fluid influenced by the pore surface; $T_{Diffusion}$ as the relaxation time of the pore fluid induced by diffusion effects.

In the context of relaxation in porous media, Brownstein and Tarr [27] also defined the fast-diffusion limit. The fast-diffusion limit states that a molecule can cross a pore multiple times during a relaxation process when the pore is small and the surface relaxation mechanism slow enough [8,21]. If the fast-diffusion limit is valid, the measured relaxation is an average of surface and bulk relaxation so that diffusion effects caused by inhomogeneities in the magnetic field may be neglected. In this case, the bulk relaxation rate is often lower than the surface relaxation rates, so that the term $\frac{1}{T_{Bulk}}$ may be neglected as well. In the case of partial saturation, relaxation rates are more strongly accelerated by surface relaxation due to surface interactions at the pore wall-liquid interface [28]. Additionally, thin water layers and the resulting liquid-air interface of partial saturated pores also result in short relaxation times [29].

Finally, with reference to the surface-to-volume ratio of a pore ($S/V$), the surface relaxation rate results in Eq. (4). At full saturation and within the fast-diffusion limit, the PSD of a sample can be obtained from a $T_1$ or $T_2$ spectrum using this equation. The material specific constant, the surface relaxivity $\rho$, thereby describes the capacity of the surface to relax the protons. Since the longitudinal and transversal relaxation represent two different processes and $S/V$ is constant within an observed pore, consequently, $\rho_1$ and $\rho_2$ differ (see (4)). Nevertheless, the surface relaxivities may be experimentally determined in multiple possible ways [21,30,31]:

1. the matching of NMR data with PSDs obtained by e.g. mercury intrusion porosimetry (MIP);
2. the use of surface area measurements (from gas adsorption or image analysis);
3. the combination of standard Carr-Purcell-Meiboom-Gill (CPMG) sequence measurements with restricted diffusion NMR [32];
4. the use of the 'decay due to diffusion in the internal field' (DDIF) concept, which is based on internal gradient fields resulting from susceptibility variations [21].

$$\frac{1}{T_{1,2}} = \frac{S}{V}\rho_{1,2} \tag{4}$$

### 2.2. Data evaluation and computation of the numerical inversion

One main task in NMR application is the data analysis. The magnetization's amplitude and the numerical inversion of the decaying signal (see Fig. 2) are in the focus of evaluation. The initial amplitude $A_0$ of the measured decay curve is thereby proportional to the proton's quantity and therefore enables the detection of moisture ingress and moisture induced damages which is interesting for the non-destructive assessment of building conditions. However, analyzing the initial amplitude, some points must be considered:

1. Since the units of the measured values are device-dependent, a calibration is needed. Therefore, the use of bulk water as a reference sample enables the theoretically exact quantification of the moisture content within the sample.
2. In practice, the loss of proton's signal within the so-called dead time of the receiving radio frequency coil (acquisition limitation) may lead to systematic deviations of the measured moisture content. Relaxation processes shorter than the time window between excitation and recording are not measurable and therefore do not contribute to the NMR signal. With reference to the above described fast-diffusion limit (s. Section 2.1), this effect mainly occurs in very small filled pores or in partially saturated pores with only a thin layer at the pore's outer circumference.
3. In inhomogeneous magnetic fields the first echos are influenced by a transient effect which causes alternating deviations in the amplitude. More details on this effect and possible corrections may be found in [33–35].

A way to analyze the whole decaying signal is a numerical inversion to achieve a spectrum (relaxation-time distribution) showing the time constants of the superposed exponential functions. As described in Blümich et al. [22], the integral of the relaxation-time distribution is equal to the initial amplitude of the decay curve and therefore equal to the proton's quantity. In relation to the previous section (2.1), at full saturated state, the time distribution of the sample also represents its PSD.

The numerical inversion mentioned above is based on multi-exponential curve fitting and is a regularized solution of a first kind Fredholm integral equation [36]. As Fordham et al. [36] explain, the NMR community typically calls this calculation the 'inverse Laplace transformation (ILT)'. That is not correct. The true ILT cannot perform a calculation of such (time) distributions. The main problem is the needed Laplace variable which has to be complex. Taking the experimental time $t$ as the Laplace variable, therefore is a contradiction, because $t$ cannot be complex. However, the true ILT is actually used for diffusion calculations to derive real time-dependent solutions [36].

Like most inversion problems in geophysics, the numerical inversion of NMR data is considered as ill-posed and vulnerable to noise (ill-conditioned) [7,37,38]. This means that noise in the data can cause significant changes in the inversion results and there is an infinite number of solutions that may fit the noise model [7]. A typical tool to avoid problems of ill-conditioning is regularization. According to McWhirter and Pike [38], Tikhonov [39] has proposed a first regularization method of ill-posed inversion problems that is based on the $L_2$-norm (least squares method). Other methods to regularize the fitting of noisy data (non-unique problem) are amplitude and curve smoothing regularization methods e.g. the s-curve criteria as mentioned by Edelmann et al.

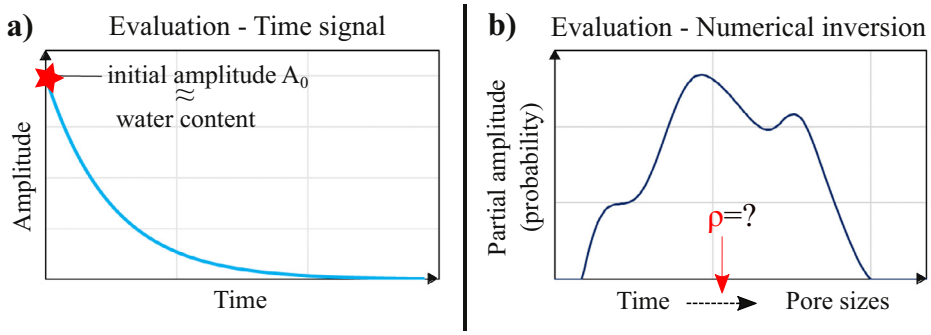


**Fig. 2.** The two main evaluation steps of NMR data analysis: determination of the proton density from the initial amplitude $A_0$ (a) and the numerical inversion to obtain a relaxation-time distribution (b); when the surface relaxivity is known, the measured relaxation times can be converted into pore sizes. *Source:* own presentation.

[37]. Positive and negative aspects of regularization and smoothing of relaxation time spectra are given by Kleinberg [40]. Furthermore, Kleinberg [40] shortly discusses the stability of multi-exponential compositions in the presence of noise.

Basics and further details on analyzing tools and inversion parameters can be found in [41–43]. Berman et al. [41] thereby deals with low-resolution NMR and shows examples of simulated and measured data. In addition, they discuss inversion results obtained with different algorithms including $L_1$ regularization (least absolute deviations method) and an optimization solver with regard to the stability and repeatability [41]. Insights into more extended practical applications of numerical inversions to obtain PSDs and surface relaxivities are given by Mohnke et al. [29], Hiller and Klitzsch [44]. While Mohnke et al. [29] used a new pore model to calculate the NMR signal of partial water fractions in pores with triangular cross sections, Hiller and Klitzsch [44] later presented a joint inversion approach to derive PSDs and surface relaxivities from NMR measurements at different capillary pressures with reference to the triangular pore model.

In the end of this section, the authors also would like to shortly mention aspects about two-dimensional (2D) distribution functions. As described in [21,22,35,45,46], multi-dimensional distribution functions (2D Laplace NMR) enable further insights into a sample compared to one-dimensional (1D) experiments. In a 2D NMR experiment, the relaxation behavior is measured in dependence of two independent variables, which can be the diffusion coefficient $D$, $T_1$ or $T_2$. For the evaluation, possible combinations of such 2D distribution functions are for example $T_1 - T_2$, $T_2 - T_2$, $D - D$ or $D - T_2$ etc. With regard to low-field NMR, 2D relaxation studies enable the determination of exchange rates between different pore systems, an analysis of heterogeneous samples and even identification of different components [35]. As explained by [47], in contrast to a $T_2$ relaxation-time distribution, 2D NMR relaxation analysis even gives information on the pore connectivity. Further advantages are its applicability within strongly imhomogeneous fields and suitability to study local internal gradients caused by susceptibility differences [22].

## 3. NMR technique development

Spectrometers that were mostly used in chemistry and biology to investigate for example silicon and polymers, were the first equipments of the NMR technique and were commercially developed in the 1950s [3–5]. Moreover, almost at the same time, NMR was implemented as a well logging tool for oil exploration since it enables a differentiation between oil and water based on the relaxation times. Within this scope, the first device to let protons precess in the earth magnetic field was designed by Varian [6]. As fascinatingly told by Lauterbur [4], afterwards, first medical applications started in the 1960s. He set up a milestone for magnetic resonance imaging (MRI) by developing a three-dimensional (3D) imaging technique based on field inhomogeneities that label the signals according to their spatial coordinates. With this development, medical investigations of humans using MRI began in the late 1970s. The first whole-body scan imaging system was then constructed in the early 1980s.

In the 1980s, as described by Clague [48], the commercial exploitation of solid-state NMR began as well. Nevertheless, first applications of dynamic NMR to cementitious materials have already been done in the late 1970s [10]. Due to the new investigation possibilities in materials research, NMR received increasing interest as a non-destructive measurement tool. Compared to other methods in materials research, namely chemical component and structure analysis, NMR is relatively easy to implement and measurements can be carried out much faster [49].

As high-resolution NMR applications require strongly homogeneous magnets (better than 0.1 ppm) with high magnetic field strength and therefore are based on large closed magnet constructions, measurable sample sizes are limited to the measurement volume within the magnet[24]. Hence, in-situ studies of large objects are not feasible and the application of high-resolution NMR is typically restricted to the laboratory [35,50,51]. An initial step for the development from MRI tomographs to handheld devices with open magnet geometries was the inside-out NMR measurement concept. This inside-out concept (called NMR logging) was developed in the oil industry and was first based on the earth's magnetic field [6,51,52]. The distinguishing feature thereby is that the entire spectrometer is inserted into the borehole as a probe. The aim of NMR logging is the determination of reservoir rock properties such as e.g. porosity, permeability, PSD, and saturation. With the commercialization of NMR logging in the 1990s and the construction of well-logging NMR sensors based on permanent magnets, finally the development and application of mobile single-sided devices was initialized [8,35,50,51].

To increase the mobility and to permit a simple handling, even on larger stationary samples on site, the development of low-field NMR in the last years clearly aimed at making NMR tools much smaller and more compact [53]. Especially for materials research and applications in the field of non-destructive testing in civil engineering, portable NMR tools are needed. Details on the development of compact NMR sensors and applications of single-sided NMR may be found in Stapf and Han [21], Casanova et al. [35], Blümich et al. [51]. Moreover, an overview about compact permanent magnet designs for portable NMR instruments is also given by Johns et al. [52], Demas and Prado [54]. Most of the developed unilateral NMR devices like the *NMR-MOUSE (Magritek Ltd)* [55,56], the surface *GARField magnet* [21,57,58] and the *NMR-MOLE* [59] have their measurement volume outside the device and are therefore not limited regarding sample geometries [53,54,60].

Single-sided devices as the *NMR-MOUSE* are normally based on permanent magnets with magnetic field strengths of around 25 mT up to 0.7 T [24]. They have a static gradient field because of their open magnet geometry and allow measurements in defined sample depths by moving the magnet. Moreover, this feature allows to carry out measurements on site [61]. As described in Nunes et al. [15], this way it is possible to investigate multilayered materials and near-surface structures (e.g. of historical buildings) non-destructively. Nevertheless, the use of

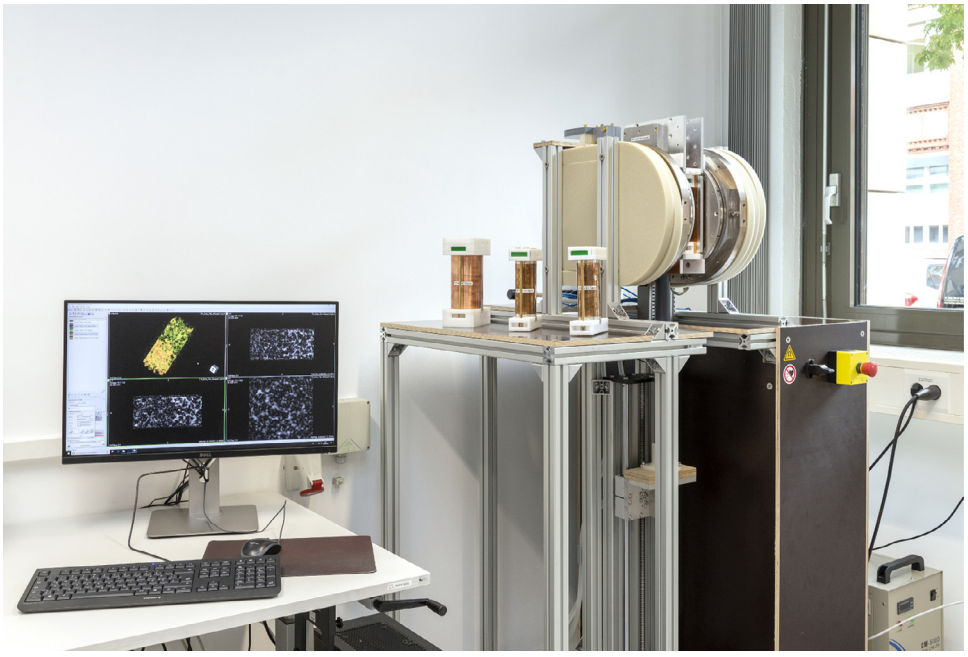

**Fig. 3.** NMR core analyzing tomograph with measuring station at *BAM*, Berlin; constructed by *Pure Devices GmbH*. *Sourcee:* BAM.

single-sided NMR devices has disadvantages. Due to the strong inhomogeneties of the magnetic field, which are caused by their geometry, one typical feature of the NMR, the chemical shift, cannot be determined. Furthermore, the transverse relaxation might be influenced by molecular self-diffusion [14,55]. However, Blümich et al. [55] explains how this drawback of diffusion effects may be used to determine constants of molecular self-diffusion.

Nowadays in the field of non-destructive testing in civil engineering, the possibility of investigating fluid transport processes over time, with high signal-to-noise ratios and in 3D, is of high significance. To better describe fast relaxation regimes (e.g. in small pores), the time window between the excitation and signal recording (echo time) must be shortened. As an example, Oligschläger et al. [53] constructed and presented the *micro-MOUSE* enabling short echo times in the range of 10 µs. With reference to the first borehole NMR tools, Oligschläger et al. [53] also presented a miniaturized inside-out NMR sensor (*DIP stick*) for moisture monitoring in any kind of construction material. The *DIP stick* has a minimal echo time of 80 µs and a measurement depth of 5 mm (distance from the magnet surface).

Besides single-sided devices, low-resolution devices as the *GeoSpec (Oxford Instruments)* [62] and the *2 MHz Rock Core Analyzer (Magritek Ltd)* [63], which fulfill the requirements of having short echo times and a more homogeneous magnetic field, are tailored to measure drill cores. To meet additional demands on new low-field NMR devices that enable e.g. slice-selective measurements in 1D, 2D and respectively 3D imaging, the company *Pure Devices GmbH* just recently constructed a core analyzing tomograph (8.97 MHz). This new device is presented in Fig. 3. It is applicable to drill cores with a maximum diameter of 72 mm (max. diameter for 3D is 42 mm). A positioning system enables measurements of long cores (more than 1 m) with a vertical resolution of 2 mm. The maximum resolution for 3D imaging is a voxel with 1 mm edge length [64].

## 4. Application tasks and examples

The NMR method represents a highly advanced tool for non-destructive testing in the field of civil engineering. For the determination of moisture contents or pore space analysis, NMR has already been applied to a high number of building materials. In the following, we give an overview about several application examples. The information is sorted by the examination material and evaluation focus (Section 2.2).

### 4.1. Detection and monitoring of moisture distributions

One main aspect of NMR measurements is the evaluation of the signal intensity (magnetization's amplitude) that is directly proportional to the hydrogen amount [25]. For this reason, the detection of the first possible signal echos is sufficient to determine the moisture content. Furthermore, relaxation-time distributions (as the result from the numerical inversion) may be used to describe and analyze moisture distributions and their dynamics. In fact, several studies exist, where moisture profiles were measured over time and sample depth, and/ or even relaxation-time distributions and their temporal development are observed.

As an example, NMR is useful to investigate the capillary absorption and dynamics of internal water content distributions [15,65]. In Gummerson et al. [65], they applied a 0.7 T NMR device to monitor the water distribution in Portland limestone, cement and in plaster bars that were sealed with an epoxy coating. To obtain a full depth profile, the authors moved the specimen step by step through the magnetically defined sensitive volume. Moisture profiles in plaster specimen and plaster-brick systems during drying processes were recorded by Nunes et al. [15]. Their object of investigation was the reduction of the water absorption coefficient by adding linseed oil as a water-repellent admixture. In particular, the use of a 0.8 T device enabled the detection of the interface between plaster and brick (sensitive slices with less than 2 mm thickness).

An example for the the study of drying processes within gypsum is given in Colinart and Glouannec [60]. The authors investigated gypsum samples with different moisture contents during drying for an in-situ study of moisture transport. For evaluation, they converted the temporal amplitude development into the related moisture contents and deduced the $T_2$ relaxation-time distributions from numerical inversions. Indeed, the results confirmed older observations of gypsum having two dominate $T_2$ times. However, during drying the shorter relaxation time remained constant while the larger time decreased [60].

A different use of NMR for industrial purpose is shown in Fleury et al. [66]. The authors used the inside-out diffusion technique to estimate the diffusion coefficient of industrial cement and concrete. In detail, they monitored the hydrogen exchange of a fully saturated sample stored in deuterium. Due to its applicability to smaller samples, this technique saves a lot of time compared to the conventional tracer test methods.

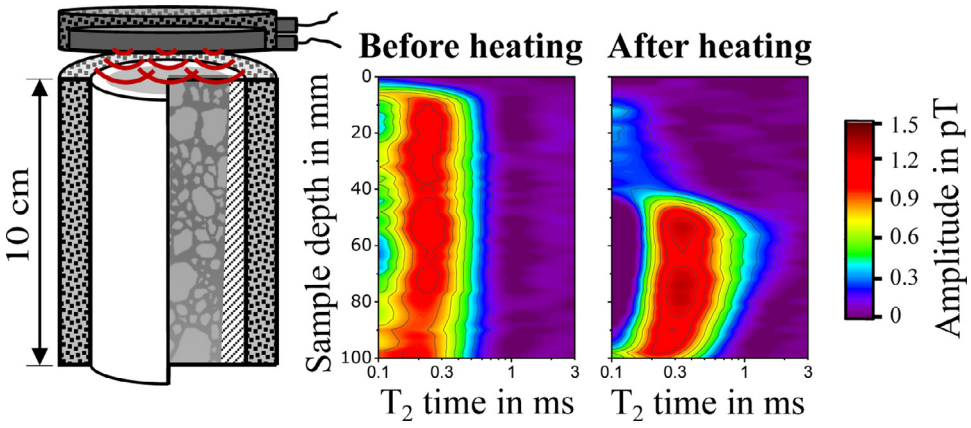


**Fig. 4.** Experimental set-up of an unilaterally-heated concrete sample and NMR relaxation-time distribution over the sample height before and after heating. *Source:* Figure adapted from [71].

Stelzner et al. [67] presented another alternative NMR application that is of high significance for civil engineering. High-performance concrete produced with and without polypropylene fibres (PP-fibres) was studied before and after heating up to 300 °C. The aim of the investigation was to better understand the thermo-hydraulic processes leading to explosive spalling during fire. Therefore, with use of the *2 MHz Rock Core Analyzer* (see Section 3), they measured the moisture content over the entire sample depth. Finally, they calculated the $T_2$ time distributions by numerical inversion. Since the magnetic gradient strength was too low to set the slice thickness of the sensitive volume to less than 2 cm when using the CPMG pulse sequence, they used a high spatial resolution approach for $T_2$ measurements [68]. This approach is based on multiple measurements with overlapping sensitive volumes which are jointly inverted. For further evaluation, the authors assumed a cut-off time ($T_2$) of 0.26 ms to distinguish between water from gel pores and interhydrate or larger pores [67]. As a result, they observed significant differences in moisture distributions before and after heating. Especially for samples including PP-fibres, the speed of the drying front appeared to be higher. Moreover, a reconfiguration of the moisture from gel pores to larger pores was indicated through the NMR results.

An exemplary result of an unilaterally-heated concrete sample is presented in Fig. 4. To analyze the redistribution of water within the concrete due to heating, the sample was measured before and dafter heating by use of the NMR tomograph at *BAM*. A full depth profile was achieved by slice-selective measurements with a slice thickness of 2 mm. The echo time was set to 70 µs. The result shows a displacement of the water front away from the heating source to the lower half within the sample. Moreover, a shift to larger relaxation times is recognizable.

Applications to wood are described in the works of Gezici-Koç et al. [69] and Casieri et al. [70]. To analyze the water content in three different kinds of wood (chestnut, walnut and sessile oak), Casieri et al. [70] used the single-sided device *EUREKA-MOUSE10* (18 MHz) produced by the *Bruker Biospin office* in Italy. The authors saturated their samples by storing them in environments having different relative humidities which were regulated by saturated saline solutions. For the gravimetric-like determination of the water content, normally the dry mass is needed. However, since the determination of the dry mass is not possible for larger objects or for valuable cultural heritage objects, they analyzed the water content by using the porosity index $I_P$. The porosity index describes the amount of water within the NMR sensitive volume and requires calibration. As a result, the authors found out that the difference in the water content determination between the gravimetric and the NMR volume fraction method depends on a factor that is related to the density of macromolecules in wood. Moreover, the authors demonstrated the potential of single-sided NMR by presenting results of measurements at a large wooden table.

Gezici-Koç et al. [69] studied pine sapwood, oak and teak by applying 1D NMR to quantify and visualize bonded and free-water distributions during water uptake and drying. Therefore, they saturated twelve samples per wood type in the same way as Casieri et al. [70] (equilibration above saturated saline solutions). One main result observed during uptake is that free water is only detectable after the filling of the cell walls. In contrast, they recorded a loss of bonded water during drying and after the vanishing of free water. Finally, the authors presented two conceptual models about diffusion (parallel and series diffusion) and found good agreement between the measured data and the so-called series diffusion model.

In the works of [69,70], they describe the same main $^1$H regimes in wood. These are the water in the cell wall, water within the lumen and water pertaining to the cellulose. Their ranges of $T_2$ relaxation times are given in Table 1. Moreover, to better distinguish the NMR signal fractions in wood, Gezici-Koç et al. [69] presented the following three possible cases of moisture distribution in wood:

1. tightly-bonded water at the cell wall (short relaxation times);
2. clusters of bonded water having an increased mobility (but no significant difference in $T_2$ time compared to case 1);
3. water within the lumen (results in large $T_2$ relaxation time).

*Observations related to hydration processes*

Besides natural stones and organic materials (e.g. woods), a big share of building materials are mineralogical composite materials such as concrete, mortar, gypsum, etc. Therefore, hydration processes play an important role in these materials so that changes in hydrogen distribution, the pore system and other material properties have to be considered. Hydration processes are complex and still not fully understood, thus many NMR monitoring applications in the laboratory focus on these processes.

A brief overview regarding the use of NMR for the analysis of hydration processes is already given in the review of Ojo and Mohr [72]. The authors point out how NMR relaxometry is useful especially for the investigation of early age cement hydration and internal curing. They explain how relative intensities and fractions of mobile and immobile water can be measured and distinguished. Furthermore, they also give insight into the influence of chemical admixtures on the cement hydration kinetics and the pore structure in early stages [72]. Another summary and collection of hydrogen applications especially in concrete research can be found in [11,12]. Although both sources only review possibilities of NMR spectroscopy, their work include various examples on how to study the degree of hydration and different states of water in fresh concrete samples.

Besides the great number of applications to cement paste and concrete, a few studies also focus on floor screed (floor finish of a maximum aggregate size of 8 mm). Edelmann et al. [37] for example investigated the moisture content in screed during the hydration process using a 22 MHz system and the *NMR-MOUSE*. Since too short relaxation times (not measurable within the instrumental dead time) and too low

**Table 1**
$T_1$ and $T_2$ relaxation times of cement and hydration components.

| Material/ Component | $T_1$ time [ms] | $T_2$ time [µs] | References ($T_1$/$T_2$) |
|---|---|---|---|
| **white cement** | | | |
| paste | 100 | 5000 | [10] |
| 1 d after hydration | ≤ 10 | ≤ 1000 | [10] |
| cement stone (dried) | 10 | 75 | [82] |
| **ordinary Portland cement** | | | |
| paste | 20 | ≤ 1000 | [10] |
| 1 d after hydration | ≤ 10 | 100 | [10] |
| **screed** (fully saturated) | | 5000–10000 | [73] |
| **gypsum** | 400 | | [82] |
| **CH phase** | 150, 600 | 20–100 | [11,82]/[77,82] |
| **C-S-H** | | | |
| interlayer water | | 20–150, 185, 500 | [77,78,82,85] |
| gel | 0.3 | | [11] |
| **alite** (shortest peak after 7 d of hydration) | 2.5 | 500 | [82] |
| **ettringite** | 10 | 10–15, 75 | [82]/[77,78,82] |
| **water** | | | |
| strongly bonded (solidlike) | | 9–20 | [72,74,81,85,86] |
| clay-bonded | | ≤ 3000 | [40] |
| within gel pores | 6 | 80–120, 300–555 | [11]]/[72,76,78,85] |
| evaporable mobil | | 40–1000 | [74,86] |
| capillary (free) | | 350, 500–$2 \cdot 10^3$, $40 \cdot 10^3$ | [72,76,85] |
| **wood** | | | |
| water in macromolecules | | 10–100 | [70] |
| cell wall water | | 100–1000 | [70] |
| water in lumen | | 10000–100000 | [70] |

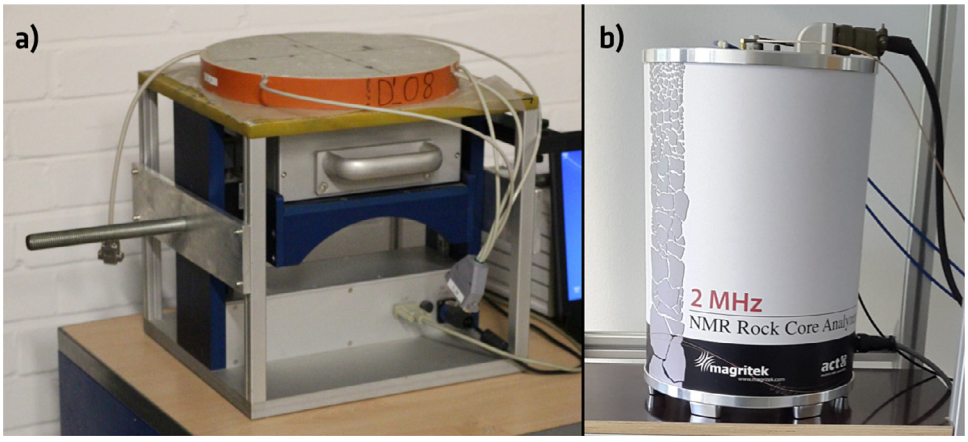


**Fig. 5.** Two NMR benchtop devices: *NMR-MOUSE* with screed sample at *BAM*. *Source:* Sabine Kruschwitz, BAM) (a) and the *2 MHz Rock Core Analyzer* at *Leibniz Institute for Applied Geophysics* (Source: Ludwig Stelzner, *BAM*) (b).

signal-to-noise ratios complicate the quantitative determination of the moisture content, the aim of this work was the definition of a reliable correlation function between the NMR signal and the moisture content in building materials.

Also using the *NMR-MOUSE*, Nagel et al. [73] measured the NMR signal of already hydrated screed samples at partial and full saturation. As a result, they discussed the changes in relaxation-time distributions at different saturation states and observed a significant shift to lower relaxation times at partial saturation. With reference to the following section, the authors also converted the relaxation times at partial saturation state to PSDs. For this purpose, the same surface relaxivity as determined at full saturation state was chosen. Furthermore, the authors investigated various diffusion effects due to field inhomogeneities of the NMR device. The observed diffusion effects occurred in synthetic materials (borosilicate plates and biobased plastic) having large pores with sizes from 1 µm up to 2.5 mm. For clarification of these diffusion effects, they did comparative measurements with the *2 MHz Rock Core Analyzer* from *Magritek Ltd*. Both used NMR devices are presented in Figure 5.

As already written above, numerous NMR measurements in materials research and civil engineering has already been carried out on cement paste and concrete. Since all hydrogen protons within cement paste or concrete are part of the added water, NMR is a helpful tool to quantify different groups of hydrogen according to their bonding and location within chemical structures [49]. In cement paste, which is described as a time-evolving porous system by Gussoni et al. [74], the state of hydrogen changes with the chemical and physical processes during hydration. Therefore, several researchers already applied NMR to cement pastes and concrete with focus on microstructures, dynamic processes, the change of proton stages, the monitoring of single components and others. The classical Portland and the white cement are often objects of research [49,65,74–79]. However, the latter is more frequently investigated, since it contains less paramagnetic impurities than the classical grey Portland cement. As explained in [22,80], such paramagnetic impurities may lead to a shortening of the relaxation times, which consequently may lead to a signal loss, when the resulting relaxation time is shorter than the device-specific dead time.

As an example, Gummerson et al. [65] monitored the change of the internal water distributions and their dynamics during capillary absorption in cement, but also in limestone and plaster. Investigations of the long-term behavior of white cement paste mixed with organic solvents were done by Gussoni et al. [74]. Moreover, they used NMR to monitor the dynamic processes of pore formation and cement microstructure forming. Indeed, this includes a differentiation between solid-like (chemically and physically bonded), liquid-like (trapped in pores) and

free water. Related to Gussoni et al. [74], Bligh et al. [49] examined the development of gel pores and interlayer water of calcium silicate hydrates (C-S-H) during hydration. However, in this work the influence of admixed retardants was an object of research as well.

Although the inside-out borehole principle is not fully counting as a non-destructive method, it is still used in materials research. Using the *DIP stick* (see Section 3), Oligschläger et al. [53] studied the curing of cement paste samples from inside of small boreholes. The studied samples had a different water content and contained additional amounts of sand. With regard to the spin density and the $T_2$ relaxation time, the authors identified three curing stages. The first stage takes around 15 min and is mainly influenced by free liquid water. During the second stage, which takes around 1–2 h, a slight change in $T_2$ time and spin density is measurable. The third stage finally shows a large reduction of the $T_2$ time and spin density.

A method how to distinguish between different hydrogen groups (e.g. intra- and inter C-S-H gel pore water) in white cement paste using a bench-top NMR spectrometer is presented by McDonald et al. [76]. To determine the amount of water loss and the existing hydrogen bonds, the authors analyzed the NMR signal as a function of the sample mass during controlled drying. Therefore, they dried the samples in three stages to remove successively the evaporable water from inter-C-S-H gel pores, in the next step from intra-C-S-H sheets and, in a last step, the solid-like water. Applying a single component exponential curve fitting, they obtained the signal amplitudes of the bonded and mobile hydrogen fractions [76]. The work of Jehng et al. [81] is another study related to drying processes, especially dealing with the monitoring of microstructures during wet-dry and freeze-thaw cycles.

Schulte Holthausen and Raupach [82] used the *NMR-MOUSE* (PM5) and an echo time of 30 µs. They analyzed 2D $T_1/T_2$ relaxation distributions to get a deeper insight into the NMR relaxation phenomena within cementitious porous media. Moreover, they also studied the influence of iron amounts on the relaxation process. Therefore, the authors investigated mixed cement stones (white and ordinary Portland cement) and hydrated cement phases as synthetic alite, low-iron white aluminate and synthetic ettringite. Powders of solid phases of commercial calcium hydroxide, hydrotalcite and gypsum have been measured as well. As a result, Schulte Holthausen and Raupach [82] found out that an increase of iron fractions linearly decreases the relaxation times and that the mineral brownmillerite can be used as an indicator for paramagentic impurities. Moreover, they observed unique $T_1/T_2$ ratios for single minerals. Their measured relaxation times are listed in Table 1.

Applications of NMR to distinguish between hydrogen groups in different states during hydration of white and classical Portland cement paste may also be found in [77–79]. They all resolved specific hydrogen fractions by analyzing the single component of the $T_2$ time distribution and the corresponding magnetization fractions. Nunes et al. [79] thereby analyzed NMR signals in dependence on varying water-to-cement ratios. In the work of Muller et al. [78], the authors registered a short $T_2$ time constant of 10 µs that is related to the mineral ettringite. Holly et al. [83] focuses only on one single hydration component during the white Portland cement hydration. To monitor the formation of the calcium aluminate phase to tricalcium aluminate through hydration, they used a home-built spectrometer (30 MHz). Indeed, this study is an example for in-situ real-time proton NMR.

An example for the use of $T_1 - T_2$ and $T_2 - T_2$ correlation measurements on white cement paste is given by [84]. In this work 2D correlation methods have been applied to cement for the first time. In detail, they measured Ketton white cement paste samples with and without added silica fume over the first 14 days of hydration. As a main result, they observed an off-diagonal peak in the $T_1 - T_2$ correlation map, which they interpreted as proof for chemical exchange of hydrogen between gel pores and capillaries. Moreover, the silica fume seemed to accelerate the hydration process. It disrupted the development of larger pores and reduced the exchange of hydrogen between capillaries and gel pores.

Although they applied NMR diffusometry, additional insights about challenges of NMR related to hydrating cement (especially fresh pastes) with reference to the presence of volatile water are given by Nestle et al. [10]. One aspect thereby is the typically shorter effective relaxation time in fresh pastes resulting from magnetic field inhomogeneities within the sample (susceptibility variations between grains and water)[10].

To conclude this section, we collated value ranges of $T_1$ and $T_2$ times determined in several scientific works referred to in this review (Table 1).

### 4.2. Pore space characterization and surface relaxivity determination

As in Section 2 explained, besides the NMR signal amplitude, the relaxation-time distribution obtained by numerical inversion is the second main objective of NMR measurements. Since NMR is sensitive to the confinement of the fluid in the porous material, the method is applicable to a wide range of materials for pore space analysis [14]. The motivation of pore space characterization using NMR is based on the capability to study effects of degradation, to determine adsorption properties as well as to quantify pore space parameters (e.g. porosity, S/V ratio and PSD) non-destructively [14,87]. According to Eq. (4), the surface relaxivity $\rho$ is required for calibration of the pore size-related $T_2$ relaxation-time distribution.

There are various studies using NMR for pore space characterization. One of them is the work of Gajewicz et al. [85]. They monitored the temporal evolution of porosity fractions according to $T_2$ relaxation times in white cement paste and in dependence of different drying and rewetting cycles. Another example is given by Rifai et al. [23], where the pore size of porous concrete was investigated in situ and under pressure. In detail, they discussed the limits of applicability, determined the porosity and calculated the PSD under the assumption of spherical pores. Furthermore, a comparison of PSDs obtained from X-Ray computer tomography (CT) data was shown.

Examples according to pore space characterization of sandstones are demonstrated by [13,87–90]. Kleinberg [88] analyzed the $T_2$ distributions of 48 sandstones and carbonates in dependence of the echo spacing (variation of diffusion time scaling). In most cases, his results showed a shift of magnetization to shorter times, but also a decrease of the average $T_2$ relaxation time with rising echo spacing. Moreover, a comparison of $T_1$ and $T_2$ relaxation times yielded congruent distributions. This reflects the complexity of natural pore systems so that 'single relaxation time models are not adequate to describe the full range of effects', [88]. One important effect that the author described is called 'pore coupling'. It describes the connectivity of the pores and therefore the effect of molecules diffusing (or sampling) multiple connected pores before relaxing [88,91]. In this context, Grunewald and Knight [91] studied the effect of pore coupling in the laboratory for silica gel samples that were treated with varying amounts of iron. In their work, they demonstrated how pore coupling decreases when the surface relaxivity is increased (e.g. by higher amounts of magnetic impurities). Furthermore, the authors explained that pore coupling may happen in well-connected pore systems and that relaxation-times distribution therefore 'reflects a complex averaging of the pore network', [91]. In fact, this phenomenon may lead to an underestimation of short relaxation times or rather micro pores as shown in the results of Grunewald and Knight [91].

The use of NMR for PSD evaluation is discussed by Kruschwitz et al. [13] and Zhang et al. [89]. In [89], a combination of µ-CT, spectral induced polarization (SIP) and MIP with NMR is applied to Bentheimer and Röttbacher sandstone samples to enable a full scale description of the pore systems. For correlation of the NMR data under the assumption of the capillary tube model, coincidence with µ-CT was striven for, because both methods should provide pore body sizes. In contrast, the methods MIP and SIP are assumed to characterize the pore throat sizes. Moreover, the determination of $\rho_2$ showed dependencies on the specific surface area and on contents of clay and iron-bearing minerals [89].

The work of Kruschwitz et al. [13] presents a multi-methodological approach to assess complex pore spaces by also combining NMR, SIP, MIP and µ-CT. Therefore, the authors extended the approach of [89] and investigated 9 different sandstone types, which they classified into 3 groups of SIP relaxation behavior. For the comparison of NMR data with PSDs (or partly pore-throat distributions), the surface relaxivity was generally chosen in a way that wider pore sizes within the $T_2$ distribution are congruent with the PSD from µ-CT. Their work provides a deep insight into the multi-methodological description of complex pore spaces with focus on distinguishing narrow and wide pore areas. Moreover, they also discussed the resolution limits and the method's sensitivities to pore throats and pore bodies. Finally, one main finding was the dependence of the SIP behavior on the pore-body-to-pore-throat ratio.

In the context of the conversion of NMR data to pore sizes, Borgia et al. [90] already studied the correlation of surface-to-volume measurements and relaxation data (different $T_1$ relaxation parameters) for samples with wide PSDs. They measured 77 sandstones of different origin using a 20 MHz NMR system [90]. Gas adsorption according to Brunauer, Emmett and Teller (BET) and MIP were their reference methods. As a result, the authors summed up that NMR does not enable an accurate estimation of the S/V ratios due to wide spreads of $\rho$ in natural stones. They concluded that a surface relaxivity determination in correlation with MIP data results in a value three times larger compared to using gas adsorption.

In contrast to the work of [90], Hürlimann et al. [87] showed an approach to overcome the shortcoming of the surface relaxivity determination from NMR data. Since it is impossible to determine the surface relaxivity only by use of relaxation measurements, the authors combined diffusion and relaxation measurements. Therefore, they first extracted the S/V ratio from NMR measurements of restricted diffusion. Subsequently, they were able to obtain the surface relaxivity from $T_1$ measurements. Their object of investigation was a core of Fontainebleau sandstone which was saturated with brine.

Further small deviations of the determined mean pore radius between NMR data and MIP might be caused by the pore surface roughness but also by other parameters such as the pore interconnections and the mercury contact angle [92]. In their study, Gallegos and Smith [92] focused on the method of regularization and calculation of the optimum relaxation smoothing parameter to obtain continuous PSDs from generated $T_1$ data sets with varying noise levels. Moreover, they also applied the method to porous solids (e.g. glasses) and proved the agreement with PSDs obtained from MIP measurements.

For the surface relaxivity determination, Kleinberg [40] and Liu et al. [32] presented alternative ways for estimating $\rho$ values in sand- and limestones. For 28 sandstone samples, a calibration of NMR data was done using not only MIP curves, but also water capillary pressure curves [40]. According to the previous explained method's sensitivities, the author explains that the match of MIP and NMR is not universal except there is a fixed multiplicative relationship between pore body and pore throat sizes or even no distinction. It seems as if that there is such a relation for sandstones. Kleinberg [40] determined a surface relaxivity that corresponds with values found in numerous studies. He mainly found out that clay-bonded water has a distinct $T_2$ time component shorter than 3 ms. The author concluded that the clay-bonded water is not coupled to the hydraulically-active pore water. Due to the high surface area of clay, surface area measurements (e.g. gas adsorption) depending on their resolution may be significantly influenced by this fact.

Another method of $\rho$ determination without consideration of pore surface measurements is based on the normally undesired diffusion effects that are caused by internal magnetic fields [32]. By extension of the phase encoding period (elongation of the echo time $t_e$), Liu et al. [32] detected high eigenmodes of the diffusion equation relying on internal field gradients and determined the pore lengths within a sand- and limestone sample. This experiment was carried out with two NMR systems: *Magritek's 2 MHz Rock Core Analyzer* and a prototype 64 MHz NMR Imaging System from *Cryogenic Ltd*. Finally, the surface relaxivities were determined by a 2D correlation function displayed in a $D - T_2$ map (with $D$ as the pore diameter). As a result, the authors observed different pore regimes with heterogeneous surface properties within the sandstone sample. Consequently and in contrast to the previously presented works, Liu et al. [32] assumed variations of the surface relaxivity depending on pore sizes within the pore system. For pore sizes in a range of 10 µm to 70 µm, $\rho$ was estimated to be around 30 µm/s. However, for pores with a size less than 10 µm, the authors observed increasing $\rho$ values [32]. For the limestone sample having a more homogeneous pore system, the correlation showed a linear relationship of $D$ and $T_2$; one effective $\rho$ for the whole sample was estimated to be 15 µm/s.

**Table 2**
List of surface relaxivity values $\rho_2$ of building materials and single hydration components.

| Material or hydration component | Surface relaxivity $\rho_2$ [µm/s] | References |
|---|---|---|
| **C-S-H** | | |
| gel | 5.51 | [93] |
| interlayer water | 0.9 | [82] |
| **ettringite** | 39–44 | [93] |
| **gypsum** | 6.2 | [93] |
| **white Portland cement** (dried) | 3.73 | [82] |
| **cement asphalt mortar** | 40 | [94] |
| **floor screed** | 50 | [73] |
| **carbonate** | | |
| limestone | 12–15 | [32] |
| carbonate rich rocks | 0.06–4.33 | [30] |
| Edwards Brown carbonate | 100 | [95] |
| Lueders carbonate | 45 | [95] |
| Indiana carbonate | 70 | [95] |
| Silurian dolomite | 25 | [95] |
| **sandstone** | | |
| unspecific | 0.92–7.1, 3, 25 - 30 | [32,40,90] |
| Bentheimer | 54, 65 | [13,89] |
| Cottaer | 100 | [13] |
| Fontainebleau | 16 | [87] |
| Langenauer | 40 | [13] |
| Obersulzbacher | 60 | [13] |
| Röttbacher | 105, 237 | [13,89] |
| Santa Fiora | 150 | [13] |
| Schleeriether | 200 | [13] |
| Skala | 40 | [13] |
| Udelfanger | 52 | [13] |

As the examples above show, the determination of $\rho$ is one of the main objectives when analyzing pore systems with NMR. Within this scope, the studies of Dalas et al. [93] and Schulte Holthausen and Raupach [82] are both fundamental works for surface relaxivity determination of cement hydrates (e.g. ettringite and C-S-H) and dried white Portland cement. While [93] thereby used BET results as reference, [82] determined $\rho$ by assuming a water layer thickness with the size of 0.28 nm (mono-layer) on the pore's outer circumference.

To conclude this section, we summed up all discussed surface relaxivity values in Table 2. This also includes results from screed, sandstones, etc. with values ranging from 0.06 µm/s (carbonate rich rocks) up to 237 µm/s (Röttbacher sandstone). A list of longitudinal surface relaxivity values $\rho_1$ of e.g. glass beads and silica gel can be found in Kleinberg [40].

### 4.3. (Perspective) on-site applications and investigations on cultural heritage

Although NMR is mainly described as a powerful tool for non-destructive testing, it is mostly still limited to the use in laboratories [96]. Nevertheless, a few examples exist, where single-sided NMR was already applied on site or rather used in laboratory with a more purposeful concept for field applications [14,15,61,96–98]. On site, NMR enables controlling of quality assessment of building materials (e.g. sprayed polymer concrete), investigations of degradation processes in infrastructure objects, state of conservation of cultural heritage, etc.

Regarding cultural heritage, an overview about possible NMR investigations is given in the reviews of Capitani et al. [17], Rehorn and Blümich [24], Blümich et al. [51]. Typical issues to be studied within this scope are the following: moisture ingress/ distribution, analysis of painting layer structures (thin-layer stratigraphy), effect of consolidation treatments on hydrophobic efficiency, moisture exchange after cleansing treatment, salt transport, porosity changes due to stone strengthener or evaluation of the state of degradation/ aging or generally the characterization of PSD. Besides applications of high-resolution NMR spectroscopy and MRI, the authors refer to numerous studies that applied NMR relaxometry by use of the Halbach core-scanner and portable unilateral NMR instruments. The measured objects actually vary from easel paintings, frescoes, wooden objects even to mummies [17,24]. To give more detailed examples, Rehorn and Blümich [24] explain that for the cases of easel paintings, the measurable hydrogen protons may be found in the paint binders as well as in the cleaning solvents. Stone strengthener are often used to repair weathered stones by increasing the hydrophobic behavior, but still maintain water vapor transport.

Sharma et al. [97] investigated a wet antique fresco, brick samples from a wall of ancient rome as well as sandstone samples that have been treated with stone strengtheners. Besides the non-destructive analysis of pore sizes and water distributions, the possibility of absolute contact-less measurements (here a distance of 1 mm to the fresco) is of great advantage when dealing with buildings and artifacts of high sociocultural value [7,97,99]. As a result, Sharma et al. [97] proved that even in the case of ferromagnetic contaminations, measurements with single-sided devices may be feasible.

The pore space of microporous porcelain samples was for example analyzed by Casieri et al. [14]. The author used the *SPINMASTER* (20 MHz) and for larger samples the single-sided device *EUREKA-MOUSE10* (19.8 MHz). Due to the use of a single-sided devices, they also considered the drawbacks of inhomogeneous fields (self-diffusion effects). To compensate the self-diffusion effects, they used the constant-echo-method [14].

Further issues represent conservation and consolidation treatments of cultural heritages, as they are widely used to prevent deterioration of artifacts and reduce the wettability of rocks. As shown in the work of Brizi et al. [16], NMR is also a powerful tool to study changes in petrophysical properties before and after treatment with consolidants, but also to localize the consolidation agent. Therefore, the authors combined three different NMR devices (split-coil scanner from *Agilent Technologies*, the *NMR-MOUSE* and the Halbach magnet from *Magritek Ltd*) and compared the obtained proton density profiles with their results from 2D $T_2 - T_2$ relaxation exchange experiments and the imaging. They investigated two commercial consolidants and a newly formulated mixture with the aim of evaluating the efficiency of consolidation treatments. They mainly focused on the hydrophobic properties, penetration depth and pore connectivity. As a result, they observed a homogeneous and uniform penetration of the treatment without significant changes of the pore connectivity.

Another example regarding conservation treatment is given by Oligschläger et al. [99]. They applied NMR on fresco paintings in the Herculaneum (Italy) and wall-painting samples for comparison in the laboratory. The aim was to investigate moisture transport processes (especially the estimation of diffusion coefficients) caused by environmental influences as e.g. salt accumulation and conservation treatment. This knowledge is important for setting up appropriate conservation and restoration plans. The authors observed a trend of moisture transport reduction (lower self-diffusion coefficients) with increasing salt concentration after conservation treatment. Moreover, the findings could be verified in the laboratory [99].

An exemplary use of the *NMR-MOUSE* is presented in the work of Weise et al. [61]. In their study, they investigated the degradation process alcali-silica reaction (ASR) at concrete roadways. Since the first phase of the degradation process is characterized by a dark dyeing of the edge regions of the roadway, they assumed moisture penetration to be the main cause for the dark dyeing. With ground penetration radar, the moisture ingress is first detected in large-scale and laterally. In the second step, NMR is applied on selected areas to obtain a depth-resolved moisture profile. The results showed high moisture contents in the joint areas and therefore confirmed the author's hypothesis [61]. For validation, the darr drying method was applied to additionally taken drill dust samples.

As the laboratory studies of [18,100] deal with coating systems as protection against aggressive substances and chemical attacks on infrastructural constructions made of concrete as well with the influence of steel reinforcement on NMR measurements, we also summed up these works in this section. Such coating systems, as investigated in this study, mainly consist of individual layers of polymers and therefore have individual amounts of measurable hydrogen protons [18]. As concrete constructions also mostly contain steel reinforcements, in both studies the *NMR-MOUSE* (PM5) was applied to determine the layer thickness of specially designed testing samples that include a set-up of various steel reinforcement configurations. Their main findings are:

1. The existence of steel leads to a shift of the measured profile and to an increase of the measured NMR amplitude.
2. The layer thickness determined with NMR proofed to be independent of steel reinforcements.

Moreover, Orlowsky [18] sums up different parameters (e.g. concrete cover, amount of steel, steel bar orientation) and their influence on the layer thickness measurement by NMR. Additionally to their measurements with the specifically designed testing specimen, they also showed a result of multilayer concrete coatings.

## 5. Difficulties and discrepancies of correlation of NMR data

In addition to the previously described NMR applications for pore space characterization, a few studies also give insights into related measurement difficulties and influences. Problems that might occur are signal loss and shortening of relaxation times caused by spatially varying internal gradients due to differences in the magnetic susceptibilities of the pore surface and the pore-filling fluid when exposed to a homogeneous external magnetic field [21,47]. Furthermore, iron oxides e.g. magnetite (especially in rocks and sands) may lead to such effects as well [80]. As studied by Keating and Knight [80], amounts of iron oxides in synthesized quartz sand samples may lead to an increase of the $T_2$ relaxation rate. Magnetite, for instance, can cause internal gradients which lead to diffusion effects that influence the relaxation rates. Sharma et al. [97] also briefly refers to the influence of magnetic impurities. However, in the cases of magnetic impurities, they observed a better agreement between NMR and MIP data, when an inhomogeneous field is used. In their opinion, 'a few large particles are less likely to be encountered in the thin sensitive volume [...] of a strong field gradient than in the homogeneous field [...], where signal is collected from the entire sample.', [97].

A study about the effect of mineralogy on the surface relaxivity with special regard to the amounts of ferro- and paramagnetic elements may be found in the work of Saidian and Prasad [30]. The authors measured carbonate-rich rock samples from Midden Bakken and Three Forks formations using various methods besides NMR. This included MIP, gas adsorption, bulk magnetic susceptibility, water immersion, etc. A main finding is that the assumption of a constant surface relaxivity for rocks is not accurate and the paramagnetic mineral content must be considered. In addition, the authors found a linear correlation between the surface relaxivity and the content of the mineral illite. This mineral thereby dominates the surface relaxation stronger than chlorite and pyrite, which contain high amounts of iron.

To the knowledge of Saidian and Prasad [30], one main problem of surface relaxivity estimation is the correlation of measurement techniques that are based on different mechanics and physics. An example for a deviating porosity determination is given in the work of Wang et al.

[94]. They determined the porosity of cement asphalt mortars by NMR and MIP and compared the obtained values. As a result, especially for the range of 1 nm to 100 nm, NMR led to a 1–2 % higher porosity than MIP. For a possible explanation, the author gave the following reasons:

1. The high pressure needed to intrude the mercury might destroy the pore wall and therefore causes a lower porosity in the range of smaller pores.
2. The vacuum-drying of the MIP samples can lead to shrinkage and thus causes cracks at larger pore sizes.
3. The size of the smallest measurable pores for MIP depends on the contact angle of MIP and the maximum applicable pressure.

In addition to that fact, Kleinberg [40] already emphasized that the match between especially MIP and NMR is not universal. This is due to the effect that MIP is more sensitive to pore throats while NMR normally gives information about the pore body size [21,89]. In this context, Wang et al. [94] states a pore size measuring range from 2 nm to 200 μm for NMR.

One further discrepancy in the correlation of NMR data is the assumption of a constant surface relaxivity for different pores within a medium. As described in Saidian and Prasad [30], theoretically $\rho$ varies for different pores. However, the measurement of $\rho$ in single pores is practically not measurable. As also explained by Hupfer [95], the often made assumption of a constant surface relaxivity for one sample or material is not realistic. Therefore, Benavides et al. [31] presented an inversion algorithm to solve surface relaxivity estimation as a function of the $T_2$ relaxation-time distribution. In this way, for one sample a whole distribution of surface relaxivity values is determinable. The authors used μ-CT images as additional data.

Self-diffusion effects in inhomogeneous magnetic fields as well as the pore model choice for correlation and interpretation of NMR data are the more general difficulties when using NMR for pore space characterization [14,29]. In this context, Mohnke et al. [29] and Tuller et al. [101] introduced a pore model with a triangular cross section that is able to maintain residual water at partial saturation. Furthermore, the shape and size of such pore geometry has a stronger influence on the water distribution and therefore the NMR amplitude than the cylindrical capillaries have [29]. Bird et al. [102] also proved inconsistency with the commonly applied parallel-capillary tube model. The authors investigated water-filled pores within glass beads, soils and sands at different matric potentials. Eventually, the work of [102] shows that NMR is an appropriate tool for the validation of pore scale models and gives an example for the determination of PSDs from $T_1$ measurements. In detail, they applied the strayfield NMR method which is based on a static magnetic fringe field with a high gradient strength (12 $Tm^{-1}$). This in turn enables slice-selective measurements and the realization of short echo times [103].

An approach to overcome or analyze the above described difficulties (e.g. internal gradients, surface relaxivity and pore geometry estimation) represents the 2D Laplace NMR method, which is classified as an advanced level of NMR measurements in Blümich et al. [22]. For example, a $T_1 - T_2$ correlation map is useful to evaluate the heterogeneity of surface relaxivity and effects of local gradients in dependence of pore sizes. $T_2 - T_2$ exchange maps are helpful to study the exchange rate of protons between different relaxation centers and therefore give information on diffusion distances and the pore geometry.

Regarding partial saturation and the validation of pore models, the authors of this review paper currently develop an approach to distinguish between water vapour and liquid phase in partly saturated pores. For this purpose, we use NMR relaxometry and calculate water film thicknesses based on relative humidities and an assumed pore model.

## 6. Summary and outlook

This state-of-the-art article is intended to give the reader an extensive overview over the application fields of NMR relaxometry and its role for materials research and especially non-destructive testing at the present state. In this context, we gave a short introduction into the theoretical background of NMR measurements and information regarding the evaluation of NMR data. With this article we also provided detailed lists of relaxation times ($T_1, T_2$) and surface relaxivities ($\rho_2$) for a number of relevant building materials and components.

The main achievement of this review paper is the extensive compilation of NMR relaxometry applications on building materials that were summed up and thematically sorted. Our focus was set on cement, concrete, screed, but also natural stones, wood, etc. As shown in the paper, by analyzing the NMR amplitude, the water content can be precisely determined, different layers of materials in composites identified and admixture influences on the water repellency investigated. The additional interpretation of the relaxation-time distribution even enables to distinguish between different hydrogen bondings and provides information about the pore system. Various studies pointed out the importance to differentiate between solid-like, liquid-like and free water in hydrating porous systems. Moreover, some examples showed how monitoring of the pore structure development and of dynamic moisture processes are possible by the use of NMR.

For a more detailed pore space characterization, NMR enables the determination of porosity, pore sizes and estimation of the pore surface mineralogy [23,70,85]. In this scope, various authors concluded that NMR is often sensitive to pore body sizes and its use may result in deviant porosity values and PSDs compared to MIP or other methods [13,40,89,94]. However, NMR measurements allow larger sample sizes and also provide information of composition and magnetic impurities due to possible occurring diffusion effects and the resulting surface relaxivity [30,91]. We also presented studies that proved how both, $T_1$ and $T_2$ time distributions, can be used to obtain PSDs [88].

Few examples of on-site applications illustrated the advantages of NMR as a non-destructive tool for the investigation of historical and cultural artifacts, but also for condition assessment of concrete roadways. Within the scope of cultural heritage, especially the investigation of stone conservation treatments with regard to the penetration uniformity and hydrophobic behavior, the characterization of layer stratigraphy in paintings etc. are of high importance [16,17,24]. As examples for perspective on-site applications, we also referred to works on concrete coating systems and studies on the influence of steel reinforcements on single-sided NMR measurements [18,100].

Besides the descriptions of the advantages and broad application fields of low-field NMR relaxometry with focus on porous building materials, we also gave an insight into the technical development of single-sided and core-analyzing devices. Since the equipment is still expensive, most portable sensors are heavy and they enable only a penetration depth of a few millimeters, further development is needed to improve the capability for in-situ NMR measurements [53,94]. As explained in the works of Oligschläger et al. [53] and Schulte Holthausen and Raupach [96], NMR devices will become more and more tailored for specific applications. Therefore, their application will be faster, more flexible and efficient.

In our opinion, the analysis of drill cores is highly relevant for the applicability of NMR in civil engineering. Therefore, we presented a new low-field tomograph for drill core analysis [64]. This new NMR tomograph with its advanced technical possibilities finally allows high-resolution 2D and 3D imaging. Due to its positioning system and the opening on both sides of the coil, measurements of large-scale cores up to ca. 1 meter length are possible.

As an outlook, the authors of this review article are planing to use this new NMR tomograph at *BAM* to effectively study fluid transport mechanism and do further pore space characterizations. More precisely, the imaging of the capillary suction behavior in sandstones as well as the pore system from older and damaged building constructions are objects of investigation. Moreover, a focus will lay in the analysis of NMR signatures at partial saturation. Therefore, especially the short echo time of

50 µs shall enable new insights into nanometer sized pores in building materials.

Further future application fields of NMR considering concrete and polymer mortar are presented in the works of Schulte Holthausen and Weichold [98], van der Heijden et al. [104] as well as of Schulte Holthausen and Raupach [96]. As an example, NMR may be applied to monitor porosity changes in concrete after heat exposure. Further topics of investigations presented by Schulte Holthausen and Raupach [96] were the applicability of single-sided NMR for quality assessment of polymeric mortar and the determination of polymer's swelling. As the results showed a shift of $T_2$ times with increasing degree of hardening of the epoxy resins and a linear correlation between the NMR amplitude and the binder content, NMR may be also used to investigate the curing behavior of epoxy resins and to determine the binder content.

Furthermore, NMR is useful to resolve protecting layers against sulfuric acid as well as for quality assessment of a new technology for surface coating concrete [96,98]. For surface protection, layers of glass are applied by flame-spraying onto the concrete surface [98]. However, the process of flame-spraying may induce damages within the concrete. Using NMR, induced cracks may be observed which increase capillary and void porosity. In addition, due to the evaporation of physically bonded water, a decrease of gel porosity may be detectable as well [98].

Another prospective application field of NMR is fire spalling of concrete. As shown in [67,104], NMR enables the analysis of moisture transport in unilaterally-heated concrete. Within this scope, van der Heijden et al. [104] presented the first experimental proof for the build up of a moisture clog and the formation of a saturated layer by means of NMR.

As a final remark, we additionally would like to refer to the review paper of Song [7] and the outlook given in Johns et al. [52], in which the authors discussed various issues concerning theoretical aspects, instrumentation and further applications.

## Declarations of Competing Interest

None.

## Acknowledgement

This work was funded by the Bundesanstalt für Materialforschung und -prüfung. Additionally, the authors would like to thank Christian Köpp and Ludwig Stelzner for their helpful feedback.

## References

[1] F. Bloch, Nuclear induction, Phys. Rev. 70 (7–8) (1946) 460–474, doi:10.1103/physrev.70.460.
[2] E.M. Purcell, H.C. Torrey, R.V. Pound, Resonance absorption by nuclear magnetic moments in a solid, Phys. Rev. 69 (1–2) (1946) 37–38, doi:10.1103/physrev.69.37.
[3] E.D. Becker, C.L. Fisk, C.L. Khetrapal, Development of NMR: from the early beginnings to the early 1990s, eMagRes, 2007, doi:10.1002/9780470034590.emrhp0001.
[4] P. Lauterbur, One path out of many: how MRI actually began, Encycl. Nucl. Magn. Reson. (2007) 445–449, doi:10.1002/9780470034590.emrhp0107.
[5] D.E. Woessner, The early days of NMR in the Southwest, Concepts Magn. Reson. 13 (2) (2001) 77–102, doi:10.1002/1099-0534(2001)13:2<77::aid-cmr1000>3.0.co;2-c.
[6] R.H. Varian, Method and means for correlating nuclear properties of atoms and magnetic fields, U.S. Patent 2,561,490, 1951.
[7] Y.-Q. Song, Magnetic resonance of porous media (MRPM): a perspective, J. Magn. Reson. 229 (2013) 12–24, doi:10.1016/j.jmr.2012.11.010.
[8] G.R. Coates, L. Xiao, M.G. Prammer, NMR Logging — Principles and Applications, Halliburton Energy Services, Houston, 1999.
[9] E.R. Andrew, Nuclear Magnetic Resonance, Cambridge Monographs on Physics, Cambridge University Press, 1969.
[10] N. Nestle, P. Galvosas, J. Kärger, Liquid-phase self-diffusion in hydrating cement pastes — results from NMR studies and perspectives for further research, Cement Concret. Res. 37 (3) (2007) 398–413, doi:10.1016/j.cemconres.2006.02.004.
[11] H. Justnes, I. Meland, J.O. Bjoergum, J. Krane, T. Skjetne, Nuclear magnetic resonance (NMR) — a powerful tool in cement and concrete research, Adv. Cement Res. 3 (11) (1990) 105–110, doi:10.1680/adcr.1990.3.11.105.
[12] P. Colombet, A.-R. Grimmer, H. Zanni, P. Sozzani, Nuclear Magnetic Resonance Spectroscopy of Cement-Based Materials, Springer, Berlin Heidelberg, 1998.
[13] S. Kruschwitz, M. Halisch, R. Dlugosch, C. Prinz, Toward a better understanding of low-frequency electrical relaxation — an enhanced pore space characterization, Geophysics 85 (4) (2020) MR257–MR270, doi:10.1190/geo2019-0074.1.
[14] C. Casieri, F.D. Luca, P. Fantazzini, Pore-size evaluation by single-sided nuclear magnetic resonance measurements: compensation of water self-diffusion effect on transverse relaxation, J. Appl. Phys. 97 (4) (2005) 043901(01–10), doi:10.1063/1.1833572.
[15] C. Nunes, L. Pel, J. Kunecký, Z. Slížková, The influence of the pore structure on the moisture transport in lime plaster-brick systems as studied by NMR, Constr. Build. Mater. 142 (2017) 395–409, doi:10.1016/j.conbuildmat.2017.03.086.
[16] L. Brizi, M. Camaiti, V. Bortolotti, P. Fantazzini, B. Blümich, S. Haber-Pohlmeier, One and two-dimensional NMR to evaluate the performance of consolidants in porous media with a wide range of pore sizes: Applications to cultural heritage, Microporous Mesoporous Mater. 269 (2018) 186–190, doi:10.1016/j.micromeso.2017.08.014.
[17] D. Capitani, V.D. Tullio, N. Proietti, Nuclear magnetic resonance to characterize and monitor cultural heritage, Prog. Nucl. Magn. Reson.Spectrosc. 64 (2012) 29–69, doi:10.1016/j.pnmrs.2011.11.001.
[18] J. Orlowsky, Analyzing of coatings on steel — reinforced concrete elements by mobile NMR, Arch. Civ. Eng. 62 (1) (2016) 65–82, doi:10.1515/ace-2015-0052.
[19] D.D. Laukien, W.H. Tschopp, Superconducting NMR magnet design, Concepts in Magnetic Resonance 6 (4) (1994) 255–273, doi:10.1002/cmr.1820060402. 9
[20] R. Kimmich, NMR Tomography Diffusometry Relaxometry, Springer, Berlin Heidelberg, 1997, doi:10.1007/978-3-642-60582-6.
[21] NMR Imaging in Chemical Engineering, S. Stapf, S.-I. Han (Eds.), Wiley, 2005, doi:10.1002/3527607560.
[22] B. Blümich, S. Haber-Pohlmeier, W. Zia, Compact NMR, De Gruyter, Berlin, 2014, doi:10.1515/9783110266719.
[23] H. Rifai, A. Staude, D. Meinel, B. Illerhaus, G. Bruno, In-situ pore size investigations of loaded porous concrete with non-destructive methods, Cement Concret. Res. 111 (2018) 72–80, doi:10.1016/j.cemconres.2018.06.008.
[24] C. Rehorn, B. Blümich, Cultural heritage studies with mobile NMR, Angew. Chem. Int. Ed. 57 (25) (2018) 7304–7312, doi:10.1002/anie.201713009.
[25] K.-J. Dunn, D. Bergman, G. Latorraca, Nuclear Magnetic Resonance – Petrophysical and Logging Applications, Handbook of Geophysical Exploration, 32, Elsevier, Oxford, 2002.
[26] R. Kleinberg, C. Straley, W. Kenyon, R. Akkurt, S. Farooqui, Nuclear magnetic resonance of rocks: $T_1$ vs. $T_2$, in: SPE Annual Technical Conference and Exhibition, SPE 26470, Society of Petroleum Engineers, 1993, doi:10.2118/26470-MS.
[27] K.R. Brownstein, C.E. Tarr, Importance of classical diffusion in NMR studies of water in biological cells, Phys. Rev. A 19 (6) (1979) 2446–2453, doi:10.1103/physreva.19.2446.
[28] O. Mohnke, Jointly deriving NMR surface relaxivity and pore size distributions by NMR relaxation experiments on partially desaturated rocks, Water Resour. Res. 50 (6) (2014) 5309–5321, doi:10.1002/2014wr015282.
[29] O. Mohnke, R. Jorand, C. Nordlund, N. Klitzsch, Understanding NMR relaxometry of partially water-saturated rocks, Hydrol. Earth Syst. Sci. 19 (6) (2015) 2763–2773, doi:10.5194/hess-19-2763-2015.
[30] M. Saidian, M. Prasad, Effect of mineralogy on nuclear magnetic resonance surface relaxivity: a case study of Middle Bakken and Three Forks formations, Fuel 161 (2015) 197–206, doi:10.1016/j.fuel.2015.08.014.
[31] F. Benavides, R. Leiderman, A. Souza, G. Carneiro, R. Bagueira, Estimating the surface relaxivity as a function of pore size from NMR $T_2$ distributions and micro-tomographic images, Comput. Geosci. 106 (2017) 200–208, doi:10.1016/j.cageo.2017.06.016.
[32] H. Liu, M.N. d'Eurydice, S. Obruchkov, P. Galvosas, Determining pore length scales and pore surface relaxivity of rock cores by internal magnetic fields modulation at 2 MHz NMR, J. Magn. Reson. 246 (2014) 110–118, doi:10.1016/j.jmr.2014.07.005.
[33] R. Schulte Holthausen, M. Raupach, Determination of porosity and pore size distribution in concrete by single-sided $^1$H NMR — from white cement pastes to grey cement mortars, 9 20. Internationale Baustofftagung, Weimar(2018)12. - 14.09.2018.
[34] M. Hürlimann, D. Griffin, Spin Dynamics of Carr–Purcell–Meiboom–Gill-like Sequences 99 in grossly inhomogeneous $B_0$ and $B_1$ fields and application to NMR Well Logging, J. Magn. Reson. 143 (1) (2000) 120–135, doi:10.1006/jmre.1999.1967.
[35] F. Casanova, J. Perlo, B. Blümich, Single-Sided NMR, Springer, Berlin Heidelberg, 2010, doi:10.1007/978-3-642-16307-4_1.
[36] E.J. Fordham, L. Venkataramanan, J. Mitchell, A. Valori, What are, and what are not, inverse Laplace transforms, J. Basic Principles Diffus.Theory Exp. Appl. 29 (2) (2017).
[37] M. Edelmann, T. Zibold, J. Grunewald, Generalised NMR-moisture correlation function of building materials based on a capillary bundle model, Cement Concret. Res. 119 (2019) 126–131, doi:10.1016/j.cemconres.2019.02.012.
[38] J.G. McWhirter, E.R. Pike, On the numerical inversion of the Laplace transform and similar Fredholm integral equations of the first kind, J. Phys. A 11 (9) (1978) 1729–1745, doi:10.1088/0305-4470/11/9/007.
[39] A.N. Tikhonov, On the solution of ill-posed problems and the method of regularization (russian), Dokl. Akad. Nauk SSSR 151 (3) (1963) 501–504.
[40] R.L. Kleinberg, Utility of NMR $T_2$ distributions, connection with capillary pressure, clay effect, and determination of the surface relaxivity parameter $\rho_2$, Magnetic Resonance Imaging 14 (7-8) (1996) 761–767, doi:10.1016/s0730-725x(96)00161-0.
[41] P. Berman, O. Levi, Y. Parmet, M. Saunders, Z. Wiesman, Laplace inversion of low-resolution NMR relaxometry data using sparse representation methods, Concepts Magn. Reson. Part A Bridg.Educ. Res. 42 (2013) 72–88.
[42] C.T.H. Baker, Numerical solution of Fredholm integral equations of first kind, Comput. J. 7 (2) (1964) 141–148, doi:10.1093/comjnl/7.2.141.

[43] A.-M. Wazwaz, The regularization method for Fredholm integral equations of the first kind, Comput. Math. Appl. 61 (10) (2011) 2981–2986, doi:10.1016/j.camwa.2011.03.083.

[44] T. Hiller, N. Klitzsch, Joint inversion of nuclear magnetic resonance data from partially saturated rocks using a triangular pore model, Geophysics 83 (4) (2018) JM15–JM28, doi:10.1190/geo2017-0697.1.

[45] S.J. Huber, Low-Field NMR: 2D Relaxation Data Analysis and Multi-Channel System Development, Technical University of Munich, 2019 Ph.D. thesis.

[46] Y. Zhang, Spatially resolved 2D Laplace NMR, RWTH Aachen University, 2014 Ph.D. thesis.

[47] A. Valori, Characterisation of cementitious materials by $^{1}$H NMR, University of Surrey, 2009 Ph.D. thesis.

[48] A.H.D. Clague, A review of the applications of recent developments of NMR in materials science, Helvetica Phys. Acta 58 (1985) 121–138, doi:10.5169/seals-115583.

[49] M.W. Bligh, M.N. d'Eurydice, R.R. Lloyd, C.H. Arns, T.D. Waite, Investigation of early hydration dynamics and microstructural development in ordinary Portland cement using $^{1}$H NMR relaxometry and isothermal calorimetry, Cement Concret. Res. 83 (Supplement C) (2016) 131–139, doi:10.1016/j.cemconres.2016.01.007.

[50] J. Kolz, N. Goga, F. Casanova, T. Mang, B. Blümich, Spatial localization with single-sided NMR sensors, Appl. Magn. Reson. 32 (1–2) (2007) 171–184, doi:10.1007/s00723-007-0011-6.

[51] B. Blümich, J. Perlo, F. Casanova, Mobile single-sided NMR, Prog. Nucl. Magn. Reson.Spectrosc. 52 (4) (2008) 197–269, doi:10.1016/j.pnmrs.2007.10.002.

[52] Mobile NMR and MRI: Developments and Applications, in: M.L. Johns, E.O. Fridjonsson, S.J. Vogt, A. Haber (Eds.), New Developments in NMR, The Royal Soc. Chem., 2016, doi:10.1039/9781782628095.

[53] D. Oligschläger, K. Kupferschläger, T. Poschadel, J. Watzlaw, B. Blümich, Miniature mobile NMR sensors for material testing and moisture-monitoring, J. Basic Principles Diffus.Theory Exp. Appl. 22 (8) (2014) 1–25.

[54] V. Demas, P.J. Prado, Compact magnets for magnetic resonance, Concepts Magn. Reson. Part A 34A (1) (2009) 48–59, doi:10.1002/cmr.a.20131.

[55] B. Blümich, P. Blümler, G. Eidmann, A. Guthausen, R. Haken, U. Schmitz, K. Saito, G. Zimmer, The NMR-MOUSE: construction, excitation, and applications, Magn. Reson. Imaging 16 (5–6) (1998) 479–484, doi:10.1016/s0730-725x(98)00069-1.

[56] Magritek Ltd, NMR-MOUSE 13 (2020) 07.07.202005.

[57] P. Aptaker, P. McDonald, J. Mitchell, Surface GARField: a novel one-sided NMR magnet and RF probe, Magn. Reson. Imaging 25 (4) (2007) 548, doi:10.1016/j.mri.2007.01.020.

[58] P. McDonald, P. Aptaker, J. Mitchell, M. Mulheron, A unilateral NMR magnet for sub-structure analysis in the built environment: the Surface GARField, J. Magn. Reson. 185 (1) (2007) 1–11, doi:10.1016/j.jmr.2006.11.001.

[59] B. Manz, A. Coy, R. Dykstra, C. Eccles, M. Hunter, B. Parkinson, P. Callaghan, A mobile one-sided NMR sensor with a homogeneous magnetic field: the NMR-MOLE, J. Magn. Reson. 183 (1) (2006) 25–31, doi:10.1016/j.jmr.2006.07.017.

[60] T. Colinart, P. Glouannec, Investigation of drying of building materials by single-sided NMR, Energy Procedia 78 (2015) 1484–1489, doi:10.1016/j.egypro.2015.11.174.

[61] F. Weise, T. Kind, L. Stelzner, M. Wieland, Dunkelfärbung der Betonfahrbahndecke im AKR-kontext, Beton- Stahlbetonbau 113 (9) (2018) 647–655, doi:10.1002/best.201800020.

[62] Oxford Instruments, GeoSpec (2020) 30.04.2020 11:20.

[63] Magritek Ltd., 2 MHz NMR Rock Core Analyzer(2020)30.04.2020 12:45.

[64] Pure Devices GmbH, MR-CAT – Core Analyzing Tomograph(2020) 02.03.2020 10:10.

[65] R.J. Gummerson, C. Hall, W.D. Hoff, R. Hawkes, G.N. Holland, W.S. Moore, Unsaturated water flow within porous materials observed by NMR imaging, Nature 281 (5726) (1979) 56–57, doi:10.1038/281056a0.

[66] M. Fleury, G. Berthe, T. Chevalier, Diffusion of water in industrial cement and concrete, Magn. Reson. Imaging 56 (2019) 32–36, doi:10.1016/j.mri.2018.09.010.

[67] L. Stelzner, B. Powierza, T. Oesch, R. Dlugosch, F. Weise, Thermally-induced moisture transport in high-performance concrete studied by X-ray-CT and $^{1}$H-NMR, Constr. Build. Mater. 224 (2019) 600–609, doi:10.1016/j.conbuildmat.2019.07.065.

[68] R. Dlugosch, T. Günther, T. Lukàcs, M. Müller-Petke, Localization and identification of thin oil layers using a slim-borehole nuclear magnetic resonance tool, Geophysics 81 (4) (2016) WB109–WB118, doi:10.1190/geo2015-0464.1.

[69] Ö. Gezici-Koç, S.J.F. Erich, H.P. Huinink, L.G.J. van der Ven, O.C.G. Adan, Bound and free water distribution in wood during water uptake and drying as measured by 1D magnetic resonance imaging, Cellulose 24 (2) (2016) 535–553, doi:10.1007/s10570-016-1173-x.

[70] C. Casieri, L. Senni, M. Romagnoli, U. Santamaria, F.D. Luca, Determination of moisture fraction in wood by mobile NMR device, J. Magn. Reson. 171 (2) (2004) 364–372, doi:10.1016/j.jmr.2004.09.014.

[71] L. Stelzner, S.M. Nagel, C. Strangfeld, F. Weise, S. Kruschwitz, NMR-Core analyzing TOMograph, Posterpresentation for the PhD-Day (internal event at *BAM*, 22.05.2019.

[72] J.O. Ojo, B.J. Mohr, A review of the analysis of cement hydration kinetics via $^{1}$H nuclear magnetic resonance, in: Nanotechnology in Construction 3, Springer, Berlin Heidelberg, 2009, pp. 107–112, doi:10.1007/978-3-642-00980-8_13.

[73] S.M. Nagel, C. Strangfeld, S. Kruschwitz, Determining the pore size distribution in synthetic and building materials using 1D NMR, J. Basic Principles Diffus.Theory Exp. Appl. 31 (2) (2019) 1–9.

[74] M. Gussoni, F. Greco, F. Bonazzi, A. Vezzoli, D. Botta, G. Dotelli, I.N. Sora, R. Pelosato, L. Zetta, $^{1}$H NMR spin-spin relaxation and imaging in porous systems: an application to the morphological study of white portland cement during hydration in the presence of organics, Magn. Reson. Imaging 22 (6) (2004) 877–889, doi:10.1016/j.mri.2004.01.068.

[75] L.J. Schreiner, J.C. Mactavish, L. Miljkovic, M. Pintar, R. Blinc, G. Lahajnar, D. Lasic, L.W. Reeves, NMR line shape-spin-lattice relaxation correlation study of portland cement hydration, J. Am. Ceram. Soc. 68 (1) (1985) 10–16, doi:10.1111/j.1151-2916.1985.tb15243.x.

[76] P.J. McDonald, V. Rodin, A. Valori, Characterisation of intra- and inter-C–S–H gel pore water in white cement based on an analysis of NMR signal amplitudes as a function of water content, Cement Concret. Res. 40 (12) (2010) 1656–1663, doi:10.1016/j.cemconres.2010.08.003.

[77] J. Greener, H. Peemoeller, C. Choi, R. Holly, E.J. Reardon, C.M. Hansson, M.M. Pintar, Monitoring of hydration of white cement paste with proton NMR spin-spin relaxation, J. Am. Ceram. Soc. 83 (3) (2000) 623–627, doi:10.1111/j.1151-2916.2000.tb01242.x.

[78] A.C.A. Muller, K.L. Scrivener, A.M. Gajewicz, P.J. McDonald, Densification of C-S-H measured by $^{1}$H NMR relaxometry, J. Phys. Chem. C 117 (1) (2012) 403–412, doi:10.1021/jp3102964.

[79] T. Nunes, P. Bodart, E.W. Randall, The hardening of portland cement studied by $^{1}$H stray-field imaging: Influence of concentration and evaporation rate of water, in: Nuclear Magnetic Resonance Spectroscopy of Cement-Based Materials, Springer, Berlin Heidelberg, 1998, pp. 411–416, doi:10.1007/978-3-642-80432-8_35.

[80] K. Keating, R. Knight, A laboratory study to determine the effect of iron oxides on proton NMR measurements, Geophysics 72 (1) (2007) E27–E32, doi:10.1190/1.2399445.

[81] J.-Y. Jehng, D. Sprague, W. Halperin, Pore structure of hydrating cement paste by magnetic resonance relaxation analysis and freezing, Magn. Reson. Imaging 14 (7) (1996) 785–791, doi:10.1016/S0730-725X(96)00164-6.

[82] R. Schulte Holthausen, M. Raupach, A phenomenological approach on the influence of paramagnetic iron in cement stone on 2D $T_1$-$T_2$ relaxation in single-sided $^{1}$H nuclear magnetic resonance, Cement Concret. Res. 120 (2019) 279–293, doi:10.1016/j.cemconres.2019.03.027.

[83] R. Holly, H. Peemoeller, M. Zhang, E. Reardon, C.M. Hansson, Magnetic resonance in situ study of tricalcium aluminate hydration in the presence of gypsum, J. Am. Ceram. Soc. 89 (3) (2006) 1022–1027, doi:10.1111/j.1551-2916.2005.00770.x.

[84] P.J. McDonald, J.-P. Korb, J. Mitchell, L. Monteilhet, Surface relaxation and chemical exchange in hydrating cement pastes: a two-dimensional NMR relaxation study, Phys. Rev. E 72 (2005) 011409, doi:10.1103/PhysRevE.72.011409.

[85] A. Gajewicz, E. Gartner, K. Kang, P. McDonald, V. Yermakou, A $^{1}$H NMR relaxometry investigation of gel-pore drying shrinkage in cement pastes, Cement Concret. Res. 86 (2016) 12–19, doi:10.1016/j.cemconres.2016.04.013.

[86] W. Halperin, J.-Y. Jehng, Y.-Q. Song, Application of spin-spin relaxation to measurement of surface area and pore size distributions in a hydrating cement paste, Magn. Reson. Imaging 12 (2) (1994) 169–173, doi:10.1016/0730-725x(94)91509-1.

[87] M.D. Hürlimann, L.L. Latour, C.H. Sotak, Diffusion measurement in sandstone core: NMR determination of surface-to-volume ratio and surface relaxivity, Magn. Reson. Imaging 12 (2) (1994) 325–327, doi:10.1016/0730-725x(94)91548-2.

[88] R.L. Kleinberg, Pore size distributions, pore coupling, and transverse relaxation spectra of porous rocks, Magn. Reson. Imaging 12 (2) (1994) 271–274.

[89] Z. Zhang, S. Kruschwitz, A. Weller, M. Halisch, Enhanced pore space analysis by use of μ-CT, MIP, NMR, and SIP, Solid Earth 9 (6) (2018) 1225–1238, doi:10.5194/se-9-1225-2018.

[90] G.C. Borgia, R.J.S. Brown, P. Fantazzini, Nuclear magnetic resonance relaxivity and surface-to-volume ratio in porous media with a wide distribution of pore sizes, J. Appl. Phys. 79 (7) (1996) 3656–3664, doi:10.1063/1.361194.

[91] E. Grunewald, R. Knight, A laboratory study of NMR relaxation times and pore coupling in heterogeneous media, Geophysics 74 (6) (2009) E215–E221, doi:10.1190/1.3223712.

[92] D.P. Gallegos, D.M. Smith, A NMR technique for the analysis of pore structure: Determination of continuous pore size distributions, J. Colloid Interface Sci. 122 (1) (1988) 143–153, doi:10.1016/0021-9797(88)90297-4.

[93] F. Dalas, J.-P. Korb, S. Pourchet, A. Nonat, D. Rinaldi, M. Mosquet, Surface relaxivity of cement hydrates, J. Phys. Chem. C 118 (16) (2014) 8387–8396, doi:10.1021/jp500055p.

[94] Y. Wang, Q. Yuan, D. Deng, T. Ye, L. Fang, Measuring the pore structure of cement asphalt mortar by nuclear magnetic resonance, Constr. Build. Mater. 137 (2017) 450–458, doi:10.1016/j.conbuildmat.2017.01.109.

[95] S. Hupfer, Spectral induced polarisation for an enhanced pore-space characterisation and analysis of dissolution processes of carbonate rocks, Clausthal University of Technology, 2020 Ph.D. thesis, doi:10.21268/20200225-1.

[96] R. Schulte Holthausen, M. Raupach, Neue Einsatzmöglichkeiten einseitiger Kernspinresonanzmesstechnik in der Baustoffforschung, Bautechnik 95 (4) (2018) 308–315, doi:10.1002/bate.201700114.

[97] S. Sharma, F. Casanova, W. Wache, A. Segre, B. Blümich, Analysis of historical porous building materials by the NMR-MOUSE®, Magn. Reson. Imaging 21 (3–4) (2003) 249–255, doi:10.1016/s0730-725x(03)00132-2.

[98] R. Schulte Holthausen, O. Weichold, Nondestructive evaluation of thermal damage in concrete by single-sided nuclear magnetic resonance, J. Infrastruct. Syst. 23 (1) (2017) B4016006, doi:10.1061/(asce)is.1943-555x.0000320.

[99] D. Oligschläger, S. Waldow, A. Haber, W. Zia, B. Blümich, Moisture dynamics in wall paintings monitored by single-sided NMR, Magn. Reson. Chem. 53 (1) (2014) 48–57, doi:10.1002/mrc.4153.

[100] J. Orlowsky, Measuring the layer thicknesses of concrete coatings by mobile NMR – a study on the influence of steel reinforcements, Constr. Build. Mater. 27 (1) (2012) 341–349, doi:10.1016/j.conbuildmat.2011.07.039.

[101] M. Tuller, D. Or, L.M. Dudley, Adsorption and capillary condensation in porous media: liquid retention and interfacial configurations in angular pores, Water Resour. Res. 35 (7) (1999) 1949–1964, doi:10.1029/1999wr900098.
[102] N.R.A. Bird, A.R. Preston, E.W. Randall, W.R. Whalley, A.P. Whitmore, Measurement of the size distribution of water-filled pores at different matric potentials by stray field nuclear magnetic resonance, Eur. J. Soil Sci. 56 (1) (2005) 135–143, doi:10.1111/j.1351-0754.2004.00658.x.
[103] P.J. McDonald, B. Newling, Stray field Magn. Reson. Imaging, Reports on Progress in Physics 61 (11) (1998) 1441–1493, doi:10.1088/0034-4885/61/11/001.
[104] G.H.A. van der Heijden, L. Pel, O.C.G. Adan, Fire spalling of concrete, as studied by NMR, Cement Concret. Res. 42 (2) (2012) 265–271, doi:10.1016/j.cemconres.2011.09.014.